

# Masses and widths of scalar-isoscalar multi-channel resonances from data analysis

Yurii S. Surovtsev<sup>1</sup>, Petr Bydžovský<sup>2</sup>, Robert Kamiński<sup>3</sup>, Valery E. Lyubovitskij<sup>4\*</sup>, Miroslav Nagy<sup>5</sup>

<sup>1</sup> *Bogoliubov Laboratory of Theoretical Physics,  
Joint Institute for Nuclear Research,  
141 980 Dubna, Russia*

<sup>2</sup> *Nuclear Physics Institute, Czech Academy of Sciences,  
Řež near Prague 25068, Czech Republic*

<sup>3</sup> *Institute of Nuclear Physics,  
Polish Academy of Sciences, Cracow 31342, Poland*

<sup>4</sup> *Institut für Theoretische Physik, Universität Tübingen,  
Kepler Center for Astro and Particle Physics,  
Auf der Morgenstelle 14, D-72076 Tübingen, Germany*

<sup>5</sup> *Institute of Physics, Slovak Academy of Sciences,  
Bratislava 84511, Slovak Republic*

(Dated: March 8, 2013)

Peculiarities of obtaining parameters for broad multi-channel resonances from data are discussed analyzing the experimental data on processes  $\pi\pi \rightarrow \pi\pi, K\bar{K}$  in the  $I^G J^{PC} = 0^+ 0^{++}$  channel in a model-independent approach based on analyticity and unitarity and using an uniformization procedure. We show that it is possible to obtain a good description of the  $\pi\pi$  scattering data from the threshold to 1.89 GeV with parameters of resonances cited in the PDG tables as preferred. However, in this case, first, representation of the  $\pi\pi$  background is unsatisfactory; second, the data on the coupled process  $\pi\pi \rightarrow K\bar{K}$  are not well described even qualitatively above 1.15 GeV when using the resonance parameters from the only  $\pi\pi$  scattering analysis. The combined analysis of these coupled processes is needed, which is carried out satisfactorily. Then both above-indicated flaws, related to the analysis of solely the  $\pi\pi$ -scattering, are cured. The most remarkable change of parameters with respect to the values of only  $\pi\pi$  scattering analysis appears for the mass of the  $f_0(600)$  which is now in some accordance with the Weinberg prediction on the basis of mended symmetry and with an analysis using the large- $N_c$  consistency conditions between the unitarization and resonance saturation. The obtained  $\pi\pi$ -scattering length  $a_0^0$  in case when we restrict to the analysis of the  $\pi\pi$  scattering or consider so-called A-solution (with a lower mass and width of  $f_0(600)$  meson) agrees well with prediction of chiral perturbation theory (ChPT) and with data extracted at CERN by the NA48/2 Collaboration from the analysis of the  $K_{e4}$  decay and by the DIRAC Collaboration from the measurement of the  $\pi^+\pi^-$  lifetime.

PACS numbers: 11.55.Bq, 11.80.Gw, 12.39.Mk, 14.40.Cs

Keywords: coupled-channel formalism, meson-meson scattering, scalar and pseudoscalar mesons

## I. INTRODUCTION

The study of scalar mesons is very important for understanding the QCD vacuum. However, despite of the big effort devoted to studying various aspects of the problem [1] (for recent reviews see, e.g. [2–5]) a description of this mesonic sector is far from being complete. Parameters of the scalar mesons, their nature and status of some of them are still not well settled [1]. For example, applying our model-independent method in the three-channel analyses of processes  $\pi\pi \rightarrow \pi\pi, K\bar{K}$ , and  $\eta\eta$  or  $\eta\eta'$  [6, 7] we have obtained parameters of the  $f_0(600)$  and  $f_0(1500)$  which differ considerably from results of analyses which utilize other methods (mainly those based on the dispersion relations and Breit–Wigner approaches). This difference is very interesting and its reasons should be understood because our method of analysis is based only on the demand for analyticity and unitarity of the amplitude using a uniformization

---

\* On leave of absence from the Department of Physics, Tomsk State University, 634050 Tomsk, Russia

procedure. The construction of the amplitude is practically free from any dynamical (model) assumptions utilizing only the *mathematical* fact that a local behaviour of analytic functions determined on the Riemann surface is governed by the nearest singularities on all corresponding sheets. I.e., the obtained parameters of resonances can be considered as free from theoretical prejudice.

To better understand reasons for the difference in results, in this paper we have performed first the two-channel model-independent analysis only of the  $\pi\pi$  scattering data. The thing is that in our previous three-channel analysis with the uniformizing variable [6, 7] we were enforced to construct a four-sheeted model of the initial eight-sheeted Riemann surface. This we have achieved by neglecting the lowest  $\pi\pi$ -threshold branch-point which means that we have considered the nearest to the physical region semi-sheets of the initial Riemann surface. This is in the line with our approach of a consistent account of the nearest singularities on all relevant sheets. The two-channel analysis utilizes the full Riemann surface and is, therefore, free of these approximations.

In the two-channel analysis only of the  $\pi\pi$  scattering data we have obtained a good description from the threshold to 1.89 GeV with values of parameters of the  $f_0$  resonances, which are well consistent with the ones cited in the PDG tables [1] as preferred. However, it was turned out that the cross-section of the coupled process  $\pi\pi \rightarrow K\bar{K}$  is not well described even qualitatively above 1.15 GeV when using for the relevant resonances the same values of parameters. The combined analysis of these coupled processes is needed, which is carried out also satisfactorily.

In the presented combined two-channel analysis of data on processes  $\pi\pi \rightarrow \pi\pi$  and  $\pi\pi \rightarrow K\bar{K}$ , we have checked whether the results of our previous three-channel analysis [6, 7] are also obtained in the two-channel case and therefore shown whether the above-indicated assumptions are justified. It is also interesting to determine and discuss the scattering length  $a_0^0$  and slope  $b_0^0$ , related to the effective range of interaction, in the separate analyses using the alternative data on  $\pi\pi$  scattering from Refs. [8] and [9], adding the very precise NA48/2-Collaboration  $\pi\pi$ -data [10].

In Sect. II a basic formalism for our two-channel model-independent method is shown and rules for the calculation of resonance parameters discussed. Results of analyses are presented and discussed in Sect. III, first only for the  $\pi\pi$  data to clarify a consistency of our results with values of parameters from the PDG tables and then for the combined two-channel analysis, using two sets of data for the  $\pi\pi$  scattering [8, 9] and all accessible data [11] for  $\pi\pi \rightarrow K\bar{K}$ , to verify a plausibility of our assumptions in the three-channel calculations. Conclusions are provided in Sect. IV.

## II. THE COUPLED-CHANNEL FORMALISM IN UNIFORMIZING VARIABLE METHOD

Our “model-independent” method which essentially utilizes an uniformizing variable can be used without any further assumptions only for the two-channel case. In the three-channel case, some assumptions about the Riemann surface have to be made [6, 7]. In this work we consider the two-channel case.

The two-channel  $S$ -matrix is determined on the four-sheeted Riemann surface. The matrix elements  $S_{ij}$ , where  $i, j = 1(\pi\pi), 2(K\bar{K})$  denote channels, have the right-hand cuts along the real axis of the  $s$  complex plane ( $s$  is the invariant total energy squared), starting with the channel thresholds  $s_i$  ( $i = 1, 2$ ), and the left-hand cuts related to the crossed channels. The Riemann-surface sheets are numbered according to the signs of analytic continuations of the roots  $\sqrt{s - s_i}$  ( $i = 1, 2$ ) as follows: signs( $\text{Im}\sqrt{s - s_1}, \text{Im}\sqrt{s - s_2}$ ) = ++, +-, --, +- correspond to sheets I, II, III, IV.

The resonance representations on the Riemann surface are obtained from the formulas which express an analytic continuation of the  $S$ -matrix elements to unphysical sheets in terms of the matrix elements on sheet I (physical) having only resonance zeros (beyond the real axis), at least, around the physical region:

$$\begin{aligned} S_{11}^{\text{II}} &= \frac{1}{S_{11}^{\text{I}}}, & S_{11}^{\text{III}} &= \frac{S_{22}^{\text{I}}}{S_{11}^{\text{I}}S_{22}^{\text{I}} - (S_{12}^{\text{I}})^2}, & S_{11}^{\text{IV}} &= \frac{S_{11}^{\text{I}}S_{22}^{\text{I}} - (S_{12}^{\text{I}})^2}{S_{22}^{\text{I}}}, \\ S_{22}^{\text{II}} &= \frac{S_{11}^{\text{I}}S_{22}^{\text{I}} - (S_{12}^{\text{I}})^2}{S_{11}^{\text{I}}}, & S_{22}^{\text{III}} &= \frac{S_{11}^{\text{I}}}{S_{11}^{\text{I}}S_{22}^{\text{I}} - (S_{12}^{\text{I}})^2}, & S_{22}^{\text{IV}} &= \frac{1}{S_{22}^{\text{I}}}, \\ S_{12}^{\text{II}} &= \frac{iS_{12}^{\text{I}}}{S_{11}^{\text{I}}}, & S_{12}^{\text{III}} &= \frac{-S_{12}^{\text{I}}}{S_{11}^{\text{I}}S_{22}^{\text{I}} - (S_{12}^{\text{I}})^2}, & S_{12}^{\text{IV}} &= \frac{iS_{12}^{\text{I}}}{S_{22}^{\text{I}}}. \end{aligned} \quad (1)$$

Then, starting from the resonance zeros on sheet I, one can obtain an arrangement of poles and zeros of a resonance on the whole Riemann surface.

In the one-channel consideration of the elastic scattering  $1 \rightarrow 1$  the main model-independent contribution of a resonance is given by a pair of conjugate poles on sheet II and by a pair of conjugate zeros on sheet I at the same conjugate points of complex energy in  $S_{11}$ . In the two-channel consideration of the processes  $1 \rightarrow 1$  and  $1 \rightarrow 2$ , a resonance is represented by a pair of conjugate poles on sheet II and by a pair of conjugate zeros on sheet I in  $S_{11}$  and also (as it is seen from eq.(2)) by a pair of conjugate poles on sheet III and by a pair of conjugate zeros on sheet IV

at the same conjugate points of complex energy if the coupling of channels is absent ( $S_{12} = 0$ ). If a resonance decays into both channels and/or takes part in processes of exchange in the crossing channels, the coupling of channels arises ( $S_{12} \neq 0$ ). Then positions of the conjugate poles on sheet III (and of corresponding zeros on sheet IV) turn out to be shifted with respect to the positions of the zeros on sheet I. Thus we obtain a cluster of poles and zeros (the pole cluster of type **(a)**) which gives the main model-independent contribution of the corresponding two-channel resonance. Obviously, depending on nature of a resonance there are two more pole clusters: when the pair of conjugate zeros on sheet I, corresponding to the resonance, is present only in  $S_{22}$  – the pole cluster of type **(b)** – and when in each of  $S_{11}$  and  $S_{22}$  – of type **(c)**. For the resonances of type **(b)**, the pair of complex conjugate poles on sheet III is shifted relative to the pair of poles on sheet IV. For the states of type **(c)**, one must consider the corresponding two pairs of conjugate poles on sheet III.

It is clear that for calculating the resonance parameters (masses, total widths and coupling constants with channels) one must use the poles on those sheets where they are not shifted due to the coupling of channels as they respects the zero position on the physical (I) sheet. For resonances of types **(a)** and **(b)** these poles are on sheets II and IV, respectively. For resonance of type **(c)** the poles can be used on both these sheets.

Analogous consideration can be carried out in the three-channel case [12, 13]. Seven types of resonances arise there. Formulas of analytic continuations of the  $S$ -matrix elements to unphysical sheets in the general case of  $N$  channels can be found in [12]. In these cases one can see that only on the sheets with the numbers  $2^i$  ( $i = 1, \dots, N$  is the number of channel), i.e. II, IV, VIII, ..., the analytic continuations of the  $S$ -matrix elements have the form  $\propto 1/S_{ii}^I$ , where  $S_{ii}^I$  is the  $S$ -matrix elements on the physical (I) sheet. This means that the pole positions of resonances only on these sheets are at the same points of the  $s$ -plane, as the resonance zeros on the physical sheet, and are not shifted due to the coupling of channels. Therefore, *the resonance parameters should be calculated from the pole positions only on these sheets*. It seems that neglecting this fact serious misunderstandings can arise. This concerns analyses which do not consider the structure of the Riemann surface of the  $S$ -matrix and especially the analyses of the decay processes in which, as a rule, the multi-channel nature of resonances is not taken into account.

In the combined analysis of coupled processes, it is convenient to use the Le Couteur–Newton relations [14]. They express the  $S$ -matrix elements of all coupled processes in terms of the Jost matrix determinant  $d(\sqrt{s-s_1}, \dots, \sqrt{s-s_N})$  that is a real analytic function with the only square-root branch-points at  $\sqrt{s-s_\alpha} = 0$ .

A necessary and sufficient condition for existence of the multi-channel resonance is its representation by one of the types of pole clusters. In order to use the representation of resonances by the pole clusters which is very important for the wide multi-channel states, we take advantage of the fact that the amplitude is a one-valued function on the Riemann surface. To this end, a uniformizing variable is applied, which maps the Riemann surface onto a plane.

In this two-channel analysis of processes  $\pi\pi \rightarrow \pi\pi, K\bar{K}$  we applied the uniformizing variable which takes into account, in addition to the  $\pi\pi$ - and  $K\bar{K}$ -threshold branch-points, the left-hand branch-point at  $s = 0$ , related to the  $\pi\pi$  crossed channels:

$$v = \frac{m_K \sqrt{s - 4m_\pi^2} + m_\pi \sqrt{s - 4m_K^2}}{\sqrt{s(m_K^2 - m_\pi^2)}}. \quad (2)$$

It maps the four-sheeted Riemann surface with two unitary cuts and the left-hand cut onto the  $v$ -plane [15] divided into two parts by a unit circle centered at the origin. In Figure II, an uniformization  $v$ -plane for the two-channel- $\pi\pi$ -scattering amplitude is shown with the representation of resonances of types **(a)**, **(b)** and **(c)**: the Roman numerals (I, ..., IV) denote the images of the corresponding sheets; the thick line represents the physical region; the points  $i$ , 1 and  $b = \sqrt{(m_K + m_\pi)/(m_K - m_\pi)}$  correspond to the  $\pi\pi, K\bar{K}$  thresholds and  $s = \infty$ , respectively; the shaded intervals  $(-\infty, -b]$ ,  $[-b^{-1}, b^{-1}]$ ,  $[b, \infty)$  are the images of the corresponding edges of the left-hand cut. The depicted positions of poles (+) and of zeros (o) give the resonance representations of the type **(a)**, **(b)** and **(c)** in  $S_{11}$ . The resonance poles are symmetric to the corresponding zeros with respect to the unit circle that guarantees the elastic unitarity of  $\pi\pi$  scattering up to the  $K\bar{K}$  threshold. The whole picture of poles and zeros is symmetric with respect to the imaginary axis guaranteeing a property of the real analyticity of the  $S$ -matrix.

On the  $v$ -plane,  $S_{11}(v)$  has no cuts;  $S_{12}(v)$  and  $S_{22}(v)$  do have the cuts which arise from the left-hand cut on the  $s$ -plane, starting at  $s = 4(m_K^2 - m_\pi^2)$ , which is further approximated by a pole

$$d_L = v^{-4}(1 - (p - i\sqrt{1-p^2})v)^4(1 + (p + i\sqrt{1-p^2})v)^4 \quad (\text{from analysis } p = 0.903 \pm 0.0004). \quad (3)$$

The fourth power is stipulated by the following model-independent arguments. First, a pole on the real  $s$ -axis on the physical sheet in  $S_{22}$  is accompanied by a pole on sheet II at the same  $s$ -value (see eq.(2)). On the  $v$ -plane this implies the pole of second order (and also zero of the same order, symmetric to the pole with respect to the real axis). Second, for the  $s$ -channel process  $\pi\pi \rightarrow K\bar{K}$ , the crossing  $u$ - and  $t$ -channels are the  $\pi - K$  and  $\bar{\pi} - K$  scattering (exchanges in these channels give contributions on the left-hand cut). This results in the additional doubling of the multiplicity

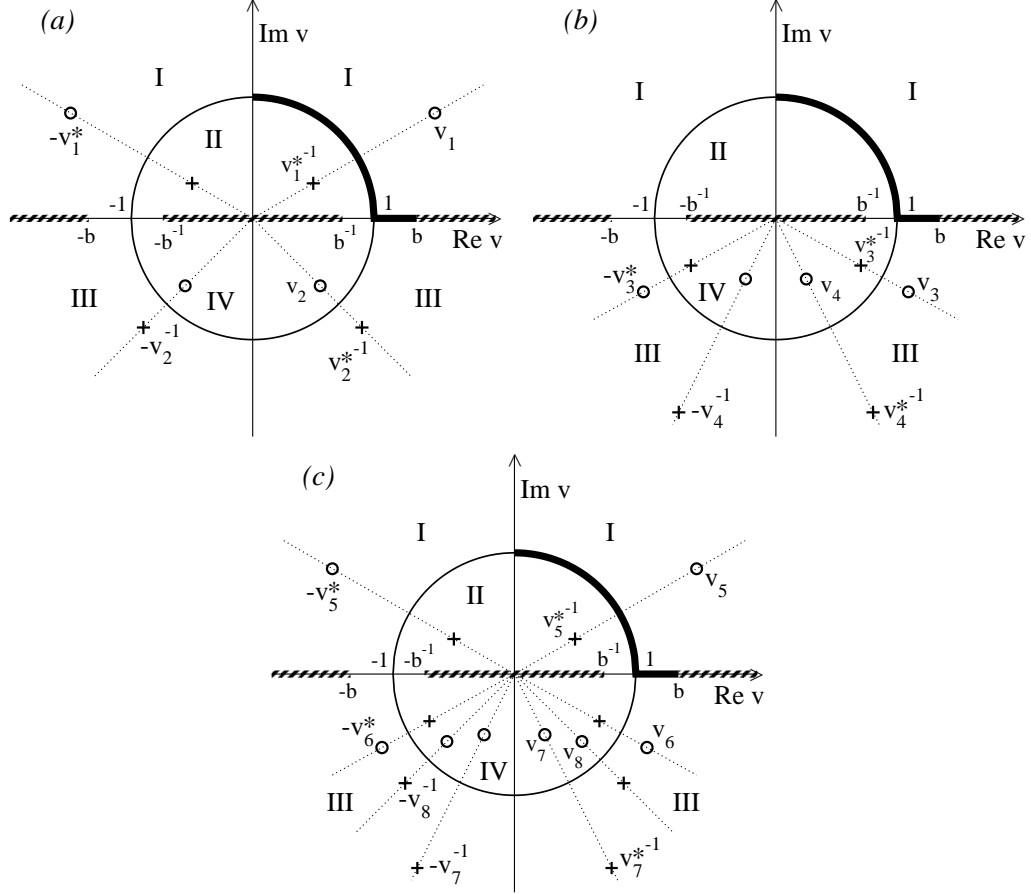


FIG. 1: Representation of resonances of type (a), (b) and (c) on the uniformization  $v$ -plane in  $S_{11}$ .

of the indicated pole on the  $v$ -plane. Therefore, the contribution of the left-hand branch-point at  $s = 4(m_K^2 - m_\pi^2)$  is approximated as the fourth-power pole on the real  $s$ -axis on the physical sheet in the sub- $K\bar{K}$ -threshold region.

On the  $v$ -plane, the Le Couteur-Newton relations are [14, 15]

$$S_{11} = \frac{d(-v^{-1})}{d(v)}, \quad S_{22} = \frac{d(v^{-1})}{d(v)}, \quad S_{11}S_{22} - S_{12}^2 = \frac{d(-v)}{d(v)}. \quad (4)$$

The main model-independent contribution of resonances, given by the pole clusters, is factorized in the  $S$ -matrix elements from the background. The possible remaining corrected and model-dependent contributions of resonances are supposed to be included in the background. Therefore the  $d(v)$ -function, which does not possess already branch points, is taken as

$$d = d_{res} d_L d_{bg}. \quad (5)$$

The function  $d_{res}(v)$  represents the contribution of resonances, described by one of three types of the pole-zero clusters, *i.e.*,

$$d_{res} = v^{-M} \prod_{n=1}^M (1 - v_n^* v)(1 + v_n v), \quad (6)$$

where  $M$  is the number of pairs of the conjugate zeros.

The background part is

$$d_{bg} = \exp\left[-i \sum_{n=1}^3 \frac{\sqrt{s - s_n}}{2m_n} (\alpha_n + i\beta_n)\right] \quad (7)$$

with

$$\alpha_n = a_{n1} + a_{n\eta} \frac{s - s_\eta}{s_\eta} \theta(s - s_\eta) + a_{n\sigma} \frac{s - s_\sigma}{s_\sigma} \theta(s - s_\sigma) + a_{nv} \frac{s - s_v}{s_v} \theta(s - s_v)$$

$$\beta_n = b_{n1} + b_{n\eta} \frac{s - s_\eta}{s_\eta} \theta(s - s_\eta) + b_{n\sigma} \frac{s - s_\sigma}{s_\sigma} \theta(s - s_\sigma) + b_{nv} \frac{s - s_v}{s_v} \theta(s - s_v)$$

where  $s_\eta$  and  $s_\sigma$  are the  $\eta\eta$  and  $\sigma\sigma$  thresholds, respectively (the latter should be determined in the analysis),  $s_v$  is a combined threshold of many opened channels in the vicinity of 1.5 GeV (e.g.,  $\eta\eta'$ ,  $\rho\rho$ ,  $\omega\omega$ ) and it is determined in the analysis:  $s_\sigma = 1.6558 \text{ GeV}^2$ ,  $s_v = 2.1293 \text{ GeV}^2$ .

The data used in the analysis are the results of phase analyses which are given for phase shifts of the amplitudes  $\delta_{\alpha\beta}$  and for modules of the  $S$ -matrix elements  $\eta_{\alpha\beta} = |S_{\alpha\beta}|$  ( $\alpha, \beta = 1, 2$ )

$$S_{\alpha\alpha} = \eta_{\alpha\alpha} e^{2i\delta_{\alpha\alpha}}, \quad S_{\alpha\beta} = \eta_{\alpha\beta} e^{i\phi_{\alpha\beta}}. \quad (8)$$

The two-channel unitarity provides the relations

$$\eta_{11} = \eta_{22}, \quad \eta_{12} = (1 - \eta_{11}^2)^{1/2}, \quad \phi_{12} = \delta_{11} + \delta_{22}. \quad (9)$$

### III. ANALYSIS OF THE DATA ON ISOSCALAR S-WAVE PROCESSES $\pi\pi \rightarrow \pi\pi, K\bar{K}$

We analyzed data on processes  $\pi\pi \rightarrow \pi\pi, K\bar{K}$ . For the  $\pi\pi$  scattering, we took alternative data – **set I**: for  $0.575 \text{ GeV} < \sqrt{s} < 1.89 \text{ GeV}$  from Ref. [8] and for  $\sqrt{s} < 1 \text{ GeV}$  from Refs. [10, 16–18, 20, 21]; **set II**: for  $0.61 \text{ GeV} < \sqrt{s} < 1.59 \text{ GeV}$  from Refs. [9] and [19] (solution G) and for  $\sqrt{s} < 1 \text{ GeV}$  as in set I. For  $\pi\pi \rightarrow K\bar{K}$ , we used practically all accessible data [11].

Initially analyzing only the  $\pi\pi$  scattering from set I, we demonstrated that it is possible to achieve an excellent description of the data for the phase shift  $\delta_{11}$  and modulus of the  $S$ -matrix element (the total  $\chi^2/\text{NDF} = 168.433/(189 - 33) \approx 1.08$ ) with the parameters of resonances (Table I) which largely coincide with the values cited as estimation of the PDG [1], though a negative phase-shift in the background on the  $\pi\pi$  threshold arises. E.g., for the  $f_0(600)$  the found pole on sheet II coincides practically with the one at around  $450 - i275 \text{ MeV}$  which was found in the recent dispersive  $\pi\pi$ -scattering data analyses [26, 27]. More remarkable differences are only for the mass of  $f_0(980)$  (1001 MeV against  $980 \pm 10 \text{ MeV}$  of PDG) and the width of  $f_0(1500)$  (336 MeV against  $109 \pm 7 \text{ MeV}$  of PDG). However, the mass of  $f_0(980)$  slightly above 1 GeV was also obtained in many other works which analyzed the  $\pi\pi$  scattering (e.g. [22]). As to the latter, we think that the observed wide resonance  $f_0(1500)$  is in reality a superposition of two states, wide and narrow. The narrow state is observed in processes considered in works cited by the PDG. To test this interpretation of the  $f_0(1500)$ , we analyzed the  $\pi\pi$ -scattering data also assuming both wide and narrow  $f_0(1500)$ . The gained description is excellent: the total  $\chi^2/\text{NDF} = 171.715/(189 - 29) \approx 1.07$ . The obtained parameters of resonances are shown in Table I. Now the parameters of the narrow  $f_0(1500)$  are consistent with those in the PDG tables. In the presented analyses, the  $f_0(600)$  and  $f_0(980)$  are described by the clusters of type (a);  $f_0(1370)$ ,  $f_0(1500)$  and  $f_0(1710)$ , type (b);  $f'_0(1500)$ , type (c). The received background parameters in the analysis with the narrow  $f_0(1500)$  are:  $a_{11} = -0.0895 \pm 0.0030$ ,  $a_{1\eta} = 0.04 \pm 0.03$ ,  $a_{1\sigma} = 0.0 \pm 0.8$ ,  $a_{1v} = 0.0 \pm 0.7$ ,  $b_{11} = 0.0 \pm 0.007$ ,  $b_{1\eta} = 0.0 \pm 0.01$ ,  $b_{1\sigma} = 0.0 \pm 0.02$ ,  $b_{1v} = 0.054 \pm 0.036$ .

In Figure 2 results of the fitting only to the  $\pi\pi$ -scattering data are shown (upper row); in the lower row there are given energy behaviours of the phase shift and module of the  $\pi\pi \rightarrow K\bar{K}$  matrix element which are calculated using the resonance parameters from the analysis of only  $\pi\pi$ -scattering: the dotted and short-dashed lines correspond to the analysis without and with the narrow  $f_0(1500)$ , respectively. The gained description of data is very good. The  $\pi\pi$  scattering length  $a_0^0$ , obtained in these analyses of the data from set I, is  $0.222 \pm 0.008 m_{\pi^+}^{-1}$ , which is also in the very good agreement with the experimental results and with the results of the ChPT calculations (see Tab. V). However, let us also emphasize two important flaws:

- First, the negative phase-shift in the background beginning from the  $\pi\pi$  threshold ( $a_{11} = -0.0895$ ) seems to be necessary for a successful description of the data. This should not be the case because, in the uniformizing variable, we have taken into account the left-hand branch-point at  $s = 0$  which gives a main contribution to the  $\pi\pi$  background below the  $K\bar{K}$  threshold. Other possible contributions of the left-hand cut related with exchanges by the nearest mesons – the  $\rho$ -meson and the  $f_0(600)$  – practically obliterate each other [15] because vector and scalar particles contribute with the opposite signs due to the gauge invariance.

TABLE I: Pole clusters for resonances on the complex energy plane  $\sqrt{s}$  in the analysis of only  $\pi\pi$ -scattering without and with the narrow  $f_0(1500)$ . Pole energies  $\sqrt{s_r} = E_r - i\Gamma_r/2$  in MeV are shown.

Without the narrow $f_0(1500)$				
Sheet		II	III	IV
$f_0(600)$	$E_r$	447.5 $\pm$ 5.4	492.6 $\pm$ 31.5	
	$\Gamma_r/2$	267.0 $\pm$ 6.2	307.8 $\pm$ 15.6	
$f_0(980)$	$E_r$	1001.1 $\pm$ 3.4	978.5 $\pm$ 9.5	
	$\Gamma_r/2$	20.3 $\pm$ 2.4	38.5 $\pm$ 6.3	
$f_0(1370)$	$E_r$		1382.6 $\pm$ 38.5	1301.2 $\pm$ 38.2
	$\Gamma_r/2$		179.5 $\pm$ 39.2	243.0 $\pm$ 52.8
$f_0(1500)$	$E_r$	1512.0 $\pm$ 10.6	1499.0 $\pm$ 108.3    1509.1 $\pm$ 112.6	1505.9 $\pm$ 30.0
	$\Gamma_r/2$	191.0 $\pm$ 10.5	310.2 $\pm$ 71.8    241.0 $\pm$ 68.9	168.0 $\pm$ 32.8
$f_0(1710)$	$E_r$		1700.3 $\pm$ 30.5	1720.1 $\pm$ 30.5
	$\Gamma_r/2$		58.8 $\pm$ 29.5	64.9 $\pm$ 34.3
With the narrow $f_0(1500)$				
Sheet		II	III	IV
$f_0(600)$	$E_r$	447.5 $\pm$ 5.9	492.7 $\pm$ 36.0	
	$\Gamma_r/2$	267.0 $\pm$ 6.5	307.8 $\pm$ 16.5	
$f_0(980)$	$E_r$	1001.1 $\pm$ 3.7	979.1 $\pm$ 12.0	
	$\Gamma_r/2$	20.3 $\pm$ 2.6	38.5 $\pm$ 7.1	
$f_0(1370)$	$E_r$		1375.8 $\pm$ 51.5	1301.1 $\pm$ 47.9
	$\Gamma_r/2$		179.5 $\pm$ 36.5	224.0 $\pm$ 49.3
$f_0(1500)$	$E_r$		1498.8 $\pm$ 39.3	1503.7 $\pm$ 45.1
	$\Gamma_r/2$		51.8 $\pm$ 43.3	56.5 $\pm$ 39.4
$f'_0(1500)$	$E_r$	1511.4 $\pm$ 11.2	1499.8 $\pm$ 104.3    1509.1 $\pm$ 119.4	1505.9 $\pm$ 38.5
	$\Gamma_r/2$	200.5 $\pm$ 11.0	310.5 $\pm$ 58.8    241.0 $\pm$ 63.8	168.1 $\pm$ 40.6
$f_0(1710)$	$E_r$		1700.3 $\pm$ 31.2	1720.1 $\pm$ 32.2
	$\Gamma_r/2$		58.6 $\pm$ 26.4	64.9 $\pm$ 30.1

- Second, the description of the data on reaction  $\pi\pi \rightarrow K\bar{K}$ , using the same parameters of resonances as in the  $\pi\pi$  channel, is satisfactory only for the phase shift  $\phi_{12}$  which is due to the approximation of the left-hand branch-point at  $s = 4(m_K^2 - m_\pi^2)$  in  $S_{12}$  and  $S_{22}$  by the fourth-power pole. The module of the  $S$ -matrix element  $\eta_{12}$  is described well only from the  $K\bar{K}$  threshold upto about 1.15 GeV as it should be due to the two-channel unitarity (see eqs. (9)). Above this energy the description fails even qualitatively (see Fig. 2).

From this we conclude that: If the data are consistent, for obtaining correct parameters of wide resonances the combined analysis of data on coupled processes is needed. Further the combined analyses of data (sets I and II) on processes  $\pi\pi \rightarrow \pi\pi, K\bar{K}$  are performed supposing that in the 1500-MeV region there are two resonances.

In the analysis of set I, the resonances are described by pole clusters of the same types as in the analysis only of  $\pi\pi$ -scattering. Satisfactory combined description of two analyzed processes is obtained with the total  $\chi^2/\text{NDF} = 391.299/(312 - 40) \approx 1.44$ . One sees that the data for the  $\pi\pi$  scattering below 1 GeV admit two solutions for the phase shift: A and B which mutually differ mainly in the pole position on sheet II for the  $f_0(600)$ . The  $\chi^2$  shown above is for the solution B. The A-solution gives a slightly worse result: the total  $\chi^2/\text{NDF} = 416.887/(312 - 40) \approx 1.53$ .

In the analysis of set II, the resonances are described by the pole clusters of the same types as in previous case except for the  $f_0(1500)$  which is represented now by the cluster of type (a) to provide more rapid growth of the  $\pi\pi$  phase shift above 1.45 GeV than in the first case.

Also in this case, a satisfactory description is obtained with the total  $\chi^2/\text{NDF} = 418.268/(306 - 41) \approx 1.58$  for the A-solution and  $\chi^2/\text{NDF} = 375.160/(306 - 41) \approx 1.42$  for the B-solution.

In Figure 3 results of the fitting to the experimental data from sets II are shown. The solid lines correspond to the A-solution and the dashed ones to the B-solution.

In Table II we show the pole clusters for resonances on the complex energy plane  $\sqrt{s}$  for the A- and B-solutions

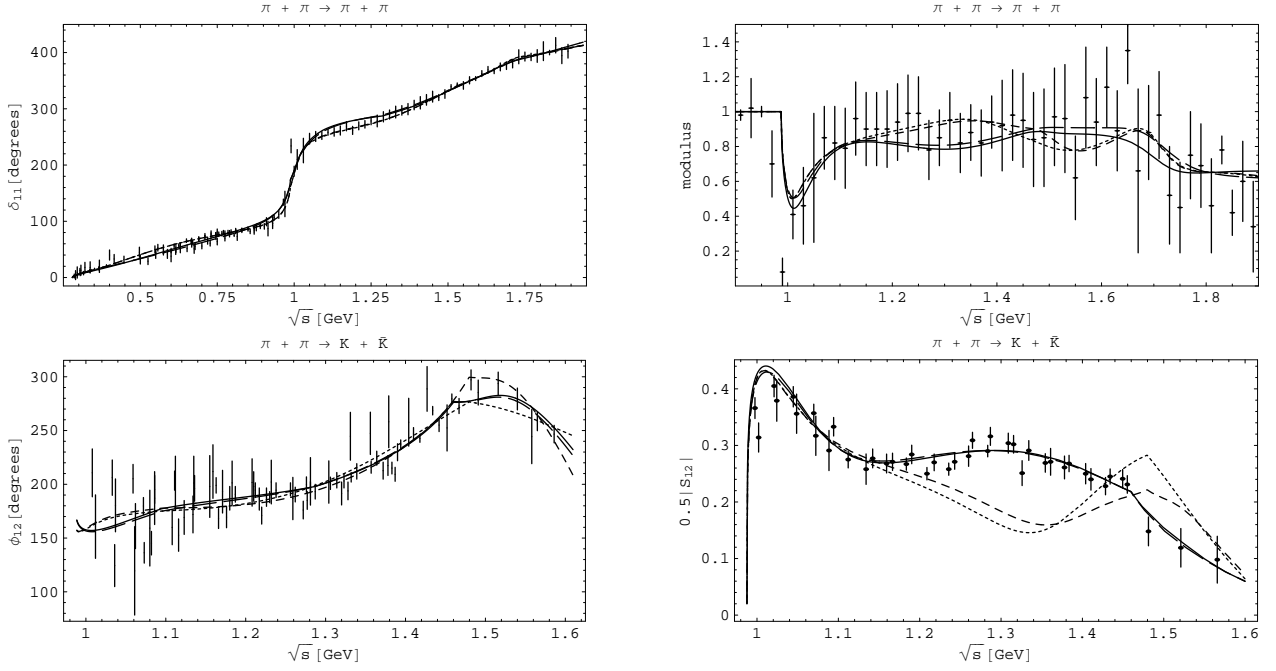


FIG. 2: The  $S$ -wave phase shifts and modules of the  $\pi\pi$ -scattering matrix element (upper row) and of the  $\pi\pi \rightarrow K\bar{K}$  matrix element in analyses of set I. The dotted and short-dashed lines correspond to the analysis of only  $\pi\pi$ -scattering without and with the narrow  $f_0(1500)$ , respectively. The long-dashed and solid lines correspond to solutions A and B of the combined analysis of  $\pi\pi \rightarrow \pi\pi, K\bar{K}$ , respectively. The data are from Refs. [8, 10, 11, 16–18, 20, 21].

in the combined analyses of data (set I) on processes  $\pi\pi \rightarrow \pi\pi, K\bar{K}$ . The obtained background parameters in the analysis of set I for the A-solution are:  $a_{11} = 0.0 \pm 0.003$ ,  $a_{1\eta} = -0.1004 \pm 0.0301$ ,  $a_{1\sigma} = 0.2148 \pm 0.0822$ ,  $a_{1v} = 0.0 \pm 0.07$ ,  $b_{11} = b_{1\eta} = b_{1\sigma} = 0$ ,  $b_{1v} = 0.012 \pm 0.0287$ ,  $a_{21} = -0.919 \pm 0.107$ ,  $a_{2\eta} = -1.399 \pm 0.348$ ,  $a_{2\sigma} = 0.0 \pm 0.7$ ,  $a_{2v} = -11.45 \pm 0.75$ ,  $b_{21} = 0.0747 \pm 0.0503$ ,  $b_{2\eta} = b_{2\sigma} = 0$ ,  $b_{2v} = 4.83 \pm 1.94$ ; for B-solution:  $a_{11} = 0.0 \pm 0.003$ ,  $a_{1\eta} = -0.0913 \pm 0.0327$ ,  $a_{1\sigma} = 0.1707 \pm 0.0899$ ,  $a_{1v} = 0.0 \pm 0.07$ ,  $b_{11} = b_{1\eta} = b_{1\sigma} = 0$ ,  $b_{1v} = 0.006 \pm 0.029$ ,  $a_{21} = -1.338 \pm 0.111$ ,  $a_{2\eta} = -1.119 \pm 0.376$ ,  $a_{2\sigma} = 0.0 \pm 0.8$ ,  $a_{2v} = -12.13 \pm 0.77$ ,  $b_{21} = 0.018 \pm 0.050$ ,  $b_{2\eta} = b_{2\sigma} = 0$ ,  $b_{2v} = 4.48 \pm 1.98$ .

It is apparent that in the combined analysis of data on coupled processes both above-indicated important flaws, which related to the analysis of only  $\pi\pi$ -scattering, are cured. Now the  $\pi\pi$  background below the  $K\bar{K}$  threshold is absent ( $a_{11} = 0.0$ ) because its contribution is practically completely accounted for by the left-hand branch-point at  $s = 0$  which is included explicitly in the uniformizing variable (2). An arising pseudo-background at the  $\eta\eta$ -threshold ( $a_{1\eta} < 0$ ) is also clear: this is a direct indication to consider explicitly the  $\eta\eta$ -threshold branch-point. This was already done in our previous work [7].

Generally, wide multi-channel states are most adequately represented by pole clusters, *i.e.*, by the poles on all the corresponding sheets, because the pole clusters give a main effect of resonances. The pole positions are rather stable characteristics for various models, whereas masses and widths are very model-dependent for wide resonances (see a discussion in Ref. [15]). Earlier one noted that the wide resonance parameters are largely controlled by the nonresonant background (see, *e.g.* [23]). In part this problem is removed due to allowing for the left-hand branch-point at  $s = 0$  in the uniformizing variable. There remains only a considerable dependence of resonance masses and widths on the used model. *E.g.*, if for the resonance part of the amplitude one use the form

$$T^{res} = \frac{\sqrt{s}\Gamma_{el}}{m_{res}^2 - s - i\sqrt{s}\Gamma_{tot}} \quad (10)$$

then masses and total widths (Tables III and IV) can be calculated using formulas

$$m_{res} = \sqrt{E_r^2 + \left(\frac{\Gamma_r}{2}\right)^2} \quad \text{and} \quad \Gamma_{tot} = \Gamma_r. \quad (11)$$

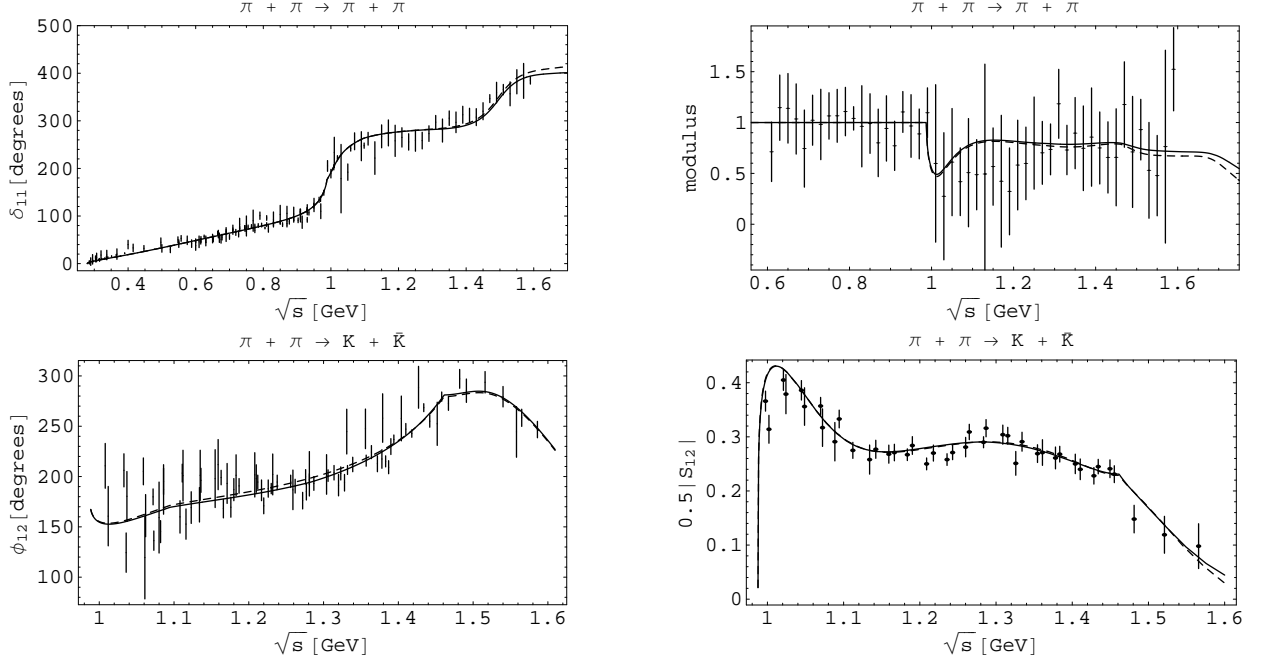


FIG. 3: The  $S$ -wave phase shifts and modules of the  $\pi\pi$ -scattering matrix element (upper row) and of the  $\pi\pi \rightarrow K\bar{K}$  matrix element in the combined analyses of the data on these two processes from set II. The solid lines correspond to the A-solution and the dashed ones to the B-solution. The data are from Refs. [9–11, 16–21].

where pole parameters  $\sqrt{s_r} = E_r - i\Gamma_r/2$  must correspond to the pole positions on sheets II and IV for the resonances of type (a), (c) and (b), respectively.

Masses and total widths of the resonances, obtained in the analyses of both sets of data (Tables III and IV), are reasonably close each other taking into account their errors.

In Table V we compare our results for the  $\pi\pi$  scattering length  $a_0^0$ , obtained in the analyses of the data of sets I and II, with results of some other theoretical and experimental works.

Let us emphasize that in the case when we limit ourselves to the analysis of the  $\pi\pi$  scattering and in the case of the scenario A (lower mass and width of  $f_0(600)$  meson) we reproduce with a high accuracy the results of the chiral perturbation theory (ChPT) [25, 26] including constraints imposed by the Roy's equations. On the other side, the solutions of the scenario B (with a heavier mass and width of  $f_0(600)$  meson) is similar to the the predictions of the chiral approaches based on the linear realization of chiral symmetry (models of the Nambu-Jona-Lasinio (NJL) type [28, 29]) Taking into account very precise experiments at CERN performed by the NA48/2 Collaboration [24] and the DIRAC Collaboration [31], which confirmed the prediction of the ChPT [25, 26] we prefer the A-solution. In particular, the NA48/2 Collaboration [24] extracted the  $S$ -wave  $\pi\pi$  scattering lengths

$$\begin{aligned} a_0^0 &= (0.2220 \pm 0.0128_{\text{stat}} \pm 0.0050_{\text{syst}} \pm 0.0037_{\text{th}}) m_{\pi^+}^{-1} \\ a_2^0 &= (-0.0432 \pm 0.0086_{\text{stat}} \pm 0.0034_{\text{syst}} \pm 0.0028_{\text{th}}) m_{\pi^+}^{-1} \end{aligned} \quad (12)$$

from the analysis of the  $K_{e4}$  decay  $K^\pm \rightarrow \pi^+\pi^-e^\pm\nu$ . The DIRAC Collaboration extracted the quantity

$$|a_0^0 - a_2^0| = \left( \left. 0.2533^{+0.0080}_{-0.0078} \right|_{\text{stat}} \left. \begin{matrix} +0.0078 \\ -0.0073 \end{matrix} \right|_{\text{syst}} \right) m_{\pi^+}^{-1} \quad (13)$$

from the measurement of the  $\pi^+\pi^-$  atom lifetime  $\tau$  in the ground state using the model-independent formula derived in Refs. [32] at next-to-leading order (NLO) in isospin breaking:

$$\tau^{-1} \sim (a_0^0 - a_2^0)^2 (1 + \delta), \quad (14)$$

where the quantity  $\delta = (5.8 \pm 1.2) \times 10^{-2}$  encodes the NLO isospin-breaking correction.



TABLE II: Pole clusters for resonances on the  $\sqrt{s}$ -plane in the combined analyses of data (set I) on processes  $\pi\pi \rightarrow \pi\pi, K\bar{K}$ .  $\sqrt{s_r} = E_r - i\Gamma_r/2$  in MeV are shown.

A-solution				
Sheet		II	III	IV
$f_0(600)$	$E_r$	$517.0 \pm 7.8$	$458.5 \pm 14.7$	
	$\Gamma_r/2$	$393.9 \pm 6.0$	$205.9 \pm 4.7$	
$f_0(980)$	$E_r$	$1004.6 \pm 3.9$	$995.5 \pm 10.1$	
	$\Gamma_r/2$	$25.0 \pm 2.3$	$96.9 \pm 2.7$	
$f_0(1370)$	$E_r$		$1351.5 \pm 32.5$	$1342.9 \pm 12.2$
	$\Gamma_r/2$		$369.0 \pm 45.7$	$221.6 \pm 30.7$
$f_0(1500)$	$E_r$		$1498.7 \pm 5.8$	$1501.1 \pm 6.4$
	$\Gamma_r/2$		$56.7 \pm 5.6$	$56.6 \pm 6.0$
$f'_0(1500)$	$E_r$	$1532.2 \pm 12.4$	$1489.1 \pm 16.2$ $1515.9 \pm 29.2$	$1519.3 \pm 18.7$
	$\Gamma_r/2$	$323.2 \pm 21.0$	$217.9 \pm 10.2$ $388.4 \pm 22.6$	$339.5 \pm 42.2$
$f_0(1710)$	$E_r$		$1701.9 \pm 31.8$	$1717.0 \pm 34.9$
	$\Gamma_r/2$		$77.8 \pm 18.0$	$72.9 \pm 16.2$
B-solution				
Sheet		II	III	IV
$f_0(600)$	$E_r$	$550.6 \pm 9.0$	$664.5 \pm 12.1$	
	$\Gamma_r/2$	$502.1 \pm 7.2$	$188.2 \pm 2.6$	
$f_0(980)$	$E_r$	$1003.2 \pm 3.0$	$995.4 \pm 7.3$	
	$\Gamma_r/2$	$28.9 \pm 2.0$	$96.7 \pm 2.7$	
$f_0(1370)$	$E_r$		$1353.8 \pm 27.9$	$1336.7 \pm 14.1$
	$\Gamma_r/2$		$367.4 \pm 37.4$	$251.9 \pm 27.5$
$f_0(1500)$	$E_r$		$1499.5 \pm 6.0$	$1500.3 \pm 6.3$
	$\Gamma_r/2$		$56.5 \pm 6.1$	$57.0 \pm 6.4$
$f'_0(1500)$	$E_r$	$1528.4 \pm 12.5$	$1491.3 \pm 15.8$ $1510.8 \pm 29.1$	$1515.6 \pm 17.0$
	$\Gamma_r/2$	$328.0 \pm 20.2$	$217.9 \pm 8.0$ $388.3 \pm 16.3$	$340.3 \pm 34.9$
$f_0(1710)$	$E_r$		$1703.1 \pm 31.5$	$1722.0 \pm 35.7$
	$\Gamma_r/2$		$81.7 \pm 19.9$	$92.3 \pm 20.3$

In Table VI we show results for the slope parameter  $b_0^0$  defined in following expansion around the threshold [27]:

$$\frac{\sqrt{s}}{4m_{\pi^+}} \sin 2\delta_{11}(s) = a_0^0 k + b_0^0 k^3 + \mathcal{O}(k^5), \quad (15)$$

where  $k = \sqrt{s/4 - m_{\pi^+}^2}$  is the pion c.m. momentum. Our results agree well with the other results only in the case of the one-channel analysis (only  $\pi\pi$  scattering). In the combined analysis the obtained values are by 20-30% smaller than the results consistent with the dispersion relations. The results do not differ so much for the A and B solutions as the scattering length.

For convenience of usage of our results, we show the positions of zeros on the  $v$ -plane, which correspond to the resonances, obtained for the solutions A: for set I –

TABLE III: Masses and total widths of the resonances, obtained in the analysis of set I.

	A-solution		B-solution	
State	$m_{res}[\text{MeV}]$	$\Gamma_{tot}[\text{MeV}]$	$m_{res}[\text{MeV}]$	$\Gamma_{tot}[\text{MeV}]$
$f_0(600)$	$650.0 \pm 9.8$	$787.8 \pm 12.0$	$745.2 \pm 11.5$	$1004.2 \pm 14.4$
$f_0(980)$	$1004.9 \pm 4.0$	$50.0 \pm 4.6$	$1003.6 \pm 3.1$	$57.8 \pm 4.0$
$f_0(1370)$	$1361.1 \pm 17.0$	$443.2 \pm 61.4$	$1360.2 \pm 18.9$	$503.8 \pm 55.0$
$f_0(1500)$	$1502.2 \pm 6.6$	$113.2 \pm 12.0$	$1501.4 \pm 6.5$	$114.0 \pm 12.8$
$f'_0(1500)$	$1565.9 \pm 16.5$	$646.4 \pm 42.0$	$1563.2 \pm 16.8$	$656.0 \pm 40.4$
$f_0(1710)$	$1718.6 \pm 35.6$	$145.8 \pm 32.4$	$1724.5 \pm 36.7$	$184.6 \pm 40.6$

TABLE IV: Masses and total widths of the resonances, obtained in the analysis of set II.

	A-solution		B-solution	
State	$m_{res}[\text{MeV}]$	$\Gamma_{tot}[\text{MeV}]$	$m_{res}[\text{MeV}]$	$\Gamma_{tot}[\text{MeV}]$
$f_0(600)$	$652.3 \pm 11.8$	$828.6 \pm 14.0$	$743.4 \pm 14.1$	$1001.8 \pm 17.4$
$f_0(980)$	$1004.4 \pm 1.8$	$54.4 \pm 3.6$	$1004.0 \pm 1.9$	$56.4 \pm 3.8$
$f_0(1370)$	$1367.8 \pm 13.5$	$444.8 \pm 53.8$	$1350.1 \pm 38.0$	$491.4 \pm 121.6$
$f_0(1500)$	$1498.7 \pm 5.3$	$113.6 \pm 9.8$	$1499.4 \pm 5.3$	$115.2 \pm 9.8$
$f'_0(1500)$	$1563.8 \pm 30.1$	$656.8 \pm 75.6$	$1564.1 \pm 29.7$	$658.8 \pm 68.4$
$f_0(1710)$	$1721.1 \pm 73.2$	$223.8 \pm 152.4$	$1721.3 \pm 47.1$	$223.8 \pm 105.0$

TABLE V: The  $\pi\pi$  scattering length  $a_0^0$ .

$a_0^0 \text{ } [m_{\pi^+}^{-1}]$	Remarks	References
$0.222 \pm 0.008$	Analysis only of $\pi\pi$ scattering	This paper
$0.230 \pm 0.004$	A-solution, set I	This paper: combined analysis of processes $\pi\pi \rightarrow \pi\pi, K\bar{K}$
$0.282 \pm 0.003$	B-solution, set I	
$0.226 \pm 0.004$	A-solution, set II	
$0.275 \pm 0.004$	B-solution, set II	
$0.26 \pm 0.05$	Analysis of the $K \rightarrow \pi\pi e\nu$ using Roy's equation	L.Rosselet et al. [20]
$0.24 \pm 0.09$	Analysis of $\pi^- p \rightarrow \pi^+ \pi^- n$ using the effective range formula	A.A.Bel'kov et al. [21]
$0.2220 \pm 0.0128_{\text{stat}} \pm 0.0050_{\text{syst}} \pm 0.0037_{\text{th}}$	Experiment on $K_{e4}$ decay	J.R. Batley et al. [24]
$0.220 \pm 0.005$	ChPT + Roy's equations	G. Colangelo et al. [25, 26]
$0.220 \pm 0.008$	Dispersion relations and $K_{e4}$ data	R.García-Martín et al. [27]
0.26	NJL model	M.K.Volkov [28]
0.28	Variant of the NJL model	A.N. Ivanov and N. Troitskaya [29]

TABLE VI: The  $\pi\pi$  scattering slope parameter  $b_0^0$ .

$b_0^0$ [ $m_{\pi^+}^{-3}$ ]	Remarks	References
$0.295 \pm 0.021$	Analysis only of $\pi\pi$ scattering	This paper
$0.210 \pm 0.010$	A-solution, set I	This paper: combined analysis of processes $\pi\pi \rightarrow \pi\pi, K\bar{K}$
$0.201 \pm 0.007$	B-solution, set I	
$0.209 \pm 0.011$	A-solution, set II	
$0.208 \pm 0.011$	B-solution, set II	
$0.278 \pm 0.005$	Analysis using Roy-like equations and forward dispersion relations	Garcia-Martin et al. [27]
$0.290 \pm 0.006$	Analysis using Roy's equations and forward dispersion relations	Kamiński et al. [35]

$$\begin{aligned}
\text{for } f_0(600) : \quad & v_1 = 1.3600 \pm 0.0080 + (0.3797 \pm 0.0076)i, & v_2 = 0.6660 \pm 0.0130 - (0.3254 \pm 0.0079)i, \\
\text{for } f_0(980) : \quad & v'_1 = 1.0657 \pm 0.0031 + (0.0346 \pm 0.0023)i, & v'_2 = 0.9006 \pm 0.0019 - (0.0725 \pm 0.0034)i, \\
\text{for } f_0(1370) : \quad & v_3 = -1.2331 \pm 0.0010 - (0.0419 \pm 0.0023)i, & v_4 = 0.7966 \pm 0.0011 - (0.0374 \pm 0.0020)i, \\
\text{for } f_0(1500) : \quad & v'_3 = -1.2467 \pm 0.0007 - (0.0077 \pm 0.0006)i, & v'_4 = 0.8023 \pm 0.0004 - (0.0050 \pm 0.0003)i, \\
\text{for } f'_0(1500) : \quad & v_5 = 1.2641 \pm 0.0014 + (0.0362 \pm 0.0016)i, & v_6 = -1.2643 \pm 0.0032 - (0.0386 \pm 0.0045)i, \\
& v_7 = 0.7981 \pm 0.0015 - (0.0184 \pm 0.0012)i, & v_8 = 0.7877 \pm 0.0033 - (0.0265 \pm 0.0031)i, \\
\text{for } f_0(1710) : \quad & v''_3 = -1.2701 \pm 0.0030 - (0.0062 \pm 0.0011)i, & v''_4 = 0.7881 \pm 0.0018 - (0.0042 \pm 0.0007)i;
\end{aligned}$$

for set II –

$$\begin{aligned}
\text{for } f_0(600) : \quad & v_1 = 1.3815 \pm 0.0102 + (0.3713 \pm 0.0096)i, & v_2 = 0.6360 \pm 0.0159 - (0.3286 \pm 0.0089)i, \\
\text{for } f_0(980) : \quad & v'_1 = 1.0664 \pm 0.0022 + (0.0373 \pm 0.0021)i, & v'_2 = 0.8998 \pm 0.0017 - (0.0742 \pm 0.0025)i, \\
\text{for } f_0(1370) : \quad & v_3 = -1.2342 \pm 0.0013 - (0.0413 \pm 0.0027)i, & v_4 = 0.7970 \pm 0.0012 - (0.0393 \pm 0.0025)i, \\
\text{for } f_0(1500) : \quad & v'_3 = 1.2463 \pm 0.0006 - (0.0078 \pm 0.0006)i, & v'_4 = 0.8029 \pm 0.0003 - (0.0054 \pm 0.0003)i, \\
\text{for } f'_0(1500) : \quad & v_5 = 1.2642 \pm 0.0059 + (0.0369 \pm 0.0103)i, & v_6 = -1.2640 \pm 0.0248 - (0.0389 \pm 0.0384)i, \\
& v_7 = 0.7980 \pm 0.0009 - (0.0185 \pm 0.0010)i, & v_8 = 0.7880 \pm 0.0128 - (0.0268 \pm 0.0202)i, \\
\text{for } f_0(1710) : \quad & v''_3 = -1.2708 \pm 0.0053 - (0.0095 \pm 0.0034)i, & v''_4 = 0.7884 \pm 0.0031 - (0.0041 \pm 0.0010)i.
\end{aligned}$$

#### IV. CONCLUSIONS

Before discussing the results of performed analysis, let us note that for calculating the wide resonance parameters (masses, total widths and coupling constants with channels) it is vital to use the poles on those sheets on which the poles are not shifted due to a coupling of channels because these poles respect positions of zeros on the physical sheet. These appropriate sheets are numerated by  $2^i$  ( $i = 1, \dots, N$  is the number of channel), i.e. II, IV, VIII,  $\dots$ . In this work we demonstrated this principle on the basis of analytic continuations of the  $S$ -matrix elements to unphysical sheets in the two-channel case. The general case of  $N$  channels can be found in other papers [7, 12].

It appears that neglecting the above-indicated principle can cause misunderstandings. This concerns especially the analyses which do not consider the structure of the Riemann surface of the  $S$ -matrix. For example, in literature there is a common opinion (delusion) that the resonance parameters should be calculated using resonance poles nearest to the physical region. This is right only in the one-channel case. In the multi-channel case this is not correct. It is obvious that, e.g., the resonance pole on sheet III, which is situated above the second threshold, is nearer to the physical region than the pole on sheet II from the pole cluster of the same resonance since above the  $K\bar{K}$  threshold the physical region (an upper edge of the right-hand cut) is joined directly with sheet III. Therefore, the pole on sheet III influences most strongly on the energy behaviour of the amplitude and this pole will be found in the analyses, not taking into account the structure of the Riemann surface and the representation of resonances by the pole clusters.

In our model-independent approach using the uniformizing variable, we analyzed data on isoscalar S-wave processes  $\pi\pi \rightarrow \pi\pi, K\bar{K}$  including the very precise NA48/2-Collaboration  $\pi\pi$ -data in a threshold region. Moreover, for the  $\pi\pi$  scattering the alternative data were taken: these are the data by B. Hyams et al.(1973) (set I) and by R. Kamiński et al.(2002) (set II) which are considerably different in the 0.76-GeV region and above 1.45 GeV.

It was shown that when analyzing only the  $\pi\pi$  scattering from set I, the good description of the data is achieved ( $\chi^2/\text{NDF} \approx 1.07$ ) with parameters of resonances (Table I) mainly coinciding with the ones cited as estimation of the PDG [1] (where for the  $f_0(600)$  the found pole on sheet II coincides practically with the one at around  $450 - i275$  MeV which was found in the recent dispersive  $\pi\pi$ -scattering data analyses [26, 27]). Exceptions are only the mass of  $f_0(980)$  (1001 MeV against  $980 \pm 10$  MeV of PDG) and the width of  $f_0(1500)$  (336 MeV against  $109 \pm 7$  MeV of PDG), though the most analyses, devoted to the  $\pi\pi$  scattering, found also the state  $f_0(980)$  above 1 GeV (e.g. [22]). As to the  $f_0(1500)$ , we analyzed also the  $\pi\pi$ -scattering assuming two states (narrow and wide) in this region. Description is of the same quality as in the first case. Parameters of the narrow  $f_0(1500)$  coincide with those preferred by the PDG.

However, first, the satisfactory description still does not mean that it is the adequate description. The point is that the negative phase-shift in the background arises already on the  $\pi\pi$  threshold. This is denoted as a pseudo-background. It appears to compensate for a too fast rise of the phase-shift of the amplitude, which is induced by the parameters of the  $f_0(600)$ , i.e., it indicates that these parameters are incorrect. Especially, the non zero negative phase shift is in contradiction with the expectation that in our parametrization the phase-shift in the  $\pi\pi$  background below the  $K\bar{K}$  threshold is practically zero [15] because the left-hand branch-point at  $s = 0$ , which gives a main contribution to the  $\pi\pi$  background below the  $K\bar{K}$  threshold, is included explicitly in the uniformizing variable. Other possible contributions of the left-hand cut from exchanges of the lightest mesons – the  $\rho$ -meson and the  $f_0(600)$  – practically obliterate each other because vector and scalar particles contribute with the opposite signs due to gauge invariance.

Second, a description of the process  $\pi\pi \rightarrow K\bar{K}$  with the resonance parameters obtained in the analysis of only the  $\pi\pi$  scattering is satisfactory only for the phase shift which is due to the fact that we approximate the left-hand branch-point at  $s = 4(m_K^2 - m_\pi^2)$  in  $S_{12}$  and  $S_{22}$  by the pole of the fourth power and that the pole clusters of resonances are chosen correctly. The module of the  $S$ -matrix element is described satisfactory only from the  $K\bar{K}$  threshold up to the energy about 1.15 GeV as it should be due to the two-channel unitarity (see eqs. (9)). Above this value of energy the module is not described well even qualitatively.

To this point let us also note results of our previous work [7] for the coupling constants of the  $f_0$  mesons with various channels. Despite of a preliminary character of these results, one can draw some conclusions about, e.g., the  $f_0(600)$  and  $f_0(980)$ . These states turn out to have large coupling constants with the  $K\bar{K}$  and especially  $\eta\eta$  systems, i.e., studying these states we deal with a multi-channel problem. Even if these states can not decay into the  $\eta\eta$  channel, their large coupling with the  $\eta\eta$  system should manifest itself in exchanges in the  $\pi\eta$  scattering.

It was shown in the two-channel approach to the  $\pi\pi$  scattering, that the combined analysis of the coupled processes – the  $\pi\pi$  scattering and  $\pi\pi \rightarrow K\bar{K}$  – is needed. This analysis was done for two sets of data (sets I and II) including two resonances in the 1500-MeV region. Then both above-indicated important remarks, related to the analysis only of the  $\pi\pi$ -scattering, are ruled out. In the combined analysis the parameters of the  $f_0(600)$  were changed considerably with the new values closer to those obtained in our previous three-channel analysis [7]. It was shown for the data of sets I and II, that in the region below 1 GeV, there are two solutions, A and B, related to the  $\sigma$ -meson/ $f_0(600)$  with the mass about 0.65 GeV and width about 0.8 GeV in the case A and  $m_\sigma \approx m_\rho$  and width about 1 GeV in the case B. This accords with the Weinberg prediction done on the basis of mended symmetry [30]. Moreover, this is also in agreement with a refined analysis using the large- $N_c$  consistency conditions between the unitarization and resonance saturation suggesting  $m_\rho - m_\sigma = O(N_c^{-1})$  [33].

Following a tradition, we speak here on the masses and total widths of resonances though the broad multi-channel states are represented more correctly by the pole clusters which are their model-independent characteristics (see the discussion in Sec.III) whereas the masses and widths are very model-dependent for wide resonances. Values of masses are necessary, e.g. for the mass relations of multiplets.

The obtained values for the  $\pi\pi$  scattering length for the A-solutions are in accordance with predictions of ChPT (non-linear realization of chiral symmetry), whereas the values for the B-solutions agree with predictions of chiral theory with linear realization of chiral symmetry (models of NJL type). Generally, considering only description of the analyzed processes, it is impossible for now to prefer any of these solutions. The B-solutions for set I and II describe the data slightly better, whereas the obtained  $\pi\pi$  scattering lengths for the A-solutions have more acceptable values. However, if one considers the problem of precise determination of the  $\pi\pi$  scattering length  $a_0^0$  to be solved taking into account the results of the NA48/2 Collaboration [24] and the DIRAC experiment [31] at CERN, then the A-solutions should be chosen. Therefore, our final conclusion is that the agreement of our approach with ChPT and data for the  $a_0^0$   $\pi\pi$  scattering length favors to the A-solutions for the masses and widths of the scalar resonances.

Finally, let us stress that our method is developed under the first principles such as analyticity, unitarity and Lorentz invariance, and therefore, it is free of any suppositions on dynamics except for an obvious statement that

a main model-independent contribution of resonances is given by the pole clusters and possible remaining small (model-dependent) contributions of resonances can be included in the background.

## V. ACKNOWLEDGMENTS

The authors thank Thomas Gutsche and Mikhail Ivanov for useful discussions and interest in this work. This work was supported in part by the Heisenberg-Landau Program, the RFBR grant 10-02-00368-a, the Votruba-Blokhintsev Program for Cooperation of Czech Republic with JINR (Dubna), the Grant Agency of Czech Republic (Grant No. P203/12/2126), the Grant Program of Plenipotentiary of Slovak Republic at JINR, the Slovak Scientific Grant Agency (Grant VEGA No.2/0034/09), the Bogoliubov-Infeld Program for Cooperation of Poland with JINR, by the DFG under Contract No. LY 114/2-1 and by Federal Targeted Program “Scientific and scientific-pedagogical personnel of innovative Russia” Contract No. 02.740.11.0238. This work has been partly supported by the Polish Ministry of Science and Higher Education (grant No N N202 101 368).

- 
- [1] K. Nakamura *et al.* (Particle Data Group Collaboration), J. Phys. G **37**, 075021 (2010).
  - [2] C. Amsler and N. A. Tornqvist, Phys. Rept. **389**, 61 (2004).
  - [3] D. V. Bugg, Phys. Rept. **397**, 257 (2004).
  - [4] F. E. Close and N. A. Tornqvist, J. Phys. G **28**, R249 (2002). **28**, R249 (2002).
  - [5] E. Klempt and A. Zaitsev, Phys. Rept. **454**, 1 (2007).
  - [6] Yu.S. Surovtsev, P. Bydžovský, R. Kamiński, and M. Nagy, Phys. Rev. D **81**, 016001 (2010).
  - [7] Yu.S. Surovtsev, P. Bydžovský and V.E. Lyubovitskij, Phys. Rev. D **85**, 036002 (2012).
  - [8] B. Hyams, C. Jones, P. Weilhammer, W. Blum, H. Dietl, G. Grayer, W. Koch and E. Lorenz *et al.*, Nucl. Phys. B **64**, 134 (1973) [AIP Conf. Proc. **13**, 206 (1973)]; Nucl. Phys. B **100**, 205 (1975).
  - [9] R. Kamiński, L. Leśniak and K. Rybicki, Z. Phys. C **74**, 79 (1997); Eur. Phys. J. direct C **4**, 4 (2002).
  - [10] J. R. Batley *et al.* (NA48/2 Collaboration), Eur. Phys. J. C **54**, 411 (2008).
  - [11] W. Wetzel, K. Freudenreich, F. X. Gentit, P. Muhlemann, W. Beusch, A. Birman, D. Websdale and P. Astbury *et al.*, Nucl. Phys. B **115**, 208 (1976); V. A. Polychronakos, N. M. Cason, J. M. Bishop, N. N. Biswas, V. P. Kenney, D. S. Rhines, R. C. Ruchti and W. D. Shephard *et al.*, Phys. Rev. D **19**, 1317 (1979); P. Estabrooks, Phys. Rev. D **19**, 2678 (1979); D. H. Cohen, D. S. Ayres, R. Diebold, S. L. Kramer, A. J. Pawlicki and A. B. Wicklund, Phys. Rev. D **22**, 2595 (1980); G. Costa *et al.* (Bari-Bonn-CERN-Glasgow-Liverpool-Milan-Vienna Collaboration), Nucl. Phys. B **175**, 402 (1980); A. Etkin, K. J. Foley, R. S. Longacre, W. A. Love, T. W. Morris, S. Ozaki, E. D. Platner and V. A. Polychronakos *et al.*, Phys. Rev. D **25**, 1786 (1982).
  - [12] D. Krupa, V. A. Meshcheryakov and Y. .S. Surovtsev, Nuovo Cim. A **109**, 281 (1996).
  - [13] Y. .S. Surovtsev, D. Krupa and M. Nagy, Phys. Rev. D **63**, 054024 (2001).
  - [14] K.J. Le Couteur, Proc. R. London, Ser. A **256**, 115 (1960); R.G. Newton, J. Math. Phys. **2**, 188 (1961); M. Kato, Ann. Phys. **31**, 130 (1965).
  - [15] Y. .S. Surovtsev, D. Krupa and M. Nagy, Eur. Phys. J. A **15**, 409 (2002).
  - [16] A. Zylbersztejn, P. Basile, M. Bourquin, J. P. Boymond, A. Diamant-Berger, P. Extermann, P. Kunz and R. Mermoud *et al.*, Phys. Lett. B **38**, 457 (1972). P. Sonderegger and P. Bonamy, in *Proc. 5th Int. Conference on Elementary Particles*, Lund, 1969, 372; J. R. Bensinger, A. R. Erwin, M. A. Thompson and W. D. Walker, Phys. Lett. B **36**, 134 (1971); J. P. Batou, G. Laurens and J. Reignier, Phys. Lett. B **33**, 525 (1970); Phys. Lett. B **33**, 528 (1970); P. Baillon, R. K. Carnegie, E. E. Kluge, D. W. G. S. Leith, H. L. Lynch, B. Ratcliff, B. Richter and H. H. Williams *et al.*, Phys. Lett. B **38**, 555 (1972); A. A. Kartamyshev, V. K. Makarin, K. N. Mukhin, O. O. Patarakin, M. M. Sulkovskaya and A. F. Sustavov, Pisma Zh. Eksp. Teor. Fiz. **25**, 68 (1977).
  - [17] S. D. Protopopescu, M. Alston-Garnjost, A. Barbaro-Galtieri, S. M. Flatte, J. H. Friedman, T. A. Lasinski, G. R. Lynch and M. S. Rabin *et al.*, Phys. Rev. D **7**, 1279 (1973).
  - [18] P. Estabrooks and A. D. Martin, Nucl. Phys. B **79**, 301 (1974).
  - [19] G. Grayer, B. Hyams, C. Jones, P. Schlein, P. Weilhammer, W. Blum, H. Dietl and W. Koch *et al.*, Nucl. Phys. B **75**, 189 (1974).
  - [20] L. Rosselet, P. Extermann, J. Fischer, O. Guisan, R. Mermoud, R. Sachot, A. M. Diamant-Berger and P. Bloch *et al.*, Phys. Rev. D **15**, 574 (1977).
  - [21] A. A. Belkov, S. A. Bunyatov, K. N. Mukhin, O. O. Patarakin, V. M. Sidorov, M. M. Sulkovskaya, A. F. Sustavov and V. A. Yarba, JETP Lett. **29**, 597 (1979) [Pisma Zh. Eksp. Teor. Fiz. **29**, 652 (1979)].
  - [22] R. García-Martín, R. Kamiński, R. Peláez, and J. Ruiz de Elvira, Phys. Rev. Lett. **107**, 072001 (2011).
  - [23] N. N. Achasov and G. N. Shestakov, Phys. Rev. D **49**, 5779 (1994).
  - [24] J. R. Batley *et al.* (NA48-2 Collaboration), Eur. Phys. J. C **70**, 635 (2010).
  - [25] G. Colangelo, J. Gasser and H. Leutwyler, Phys. Lett. B **488**, 261 (2000).

- [26] G. Colangelo, J. Gasser and H. Leutwyler, Nucl. Phys. B **603**, 125 (2001); B. Ananthanarayan, G. Colangelo, J. Gasser and H. Leutwyler, Phys. Rept. **353**, 207 (2001).
- [27] R. García-Martín, R. Kamiński, J.R. Peláez, and F.J. Ynduráin, Phys. Rev. D **83**, 074004 (2011).
- [28] M. K. Volkov, Sov. J. Part. Nucl. **17**, 186 (1986) [Fiz. Elem. Chast. Atom. Yadra **17**, 433 (1986)].
- [29] A. N. Ivanov and N. I. Troitskaya, Nuovo Cim. A **108**, 555 (1995).
- [30] S. Weinberg, Phys. Rev. Lett. **65**, 1177 (1990).
- [31] B. Adeva, L. Afanasyev, M. Benayoun, A. Benelli, Z. Berka, V. Brekhovskikh, G. Caragheorgheopol and T. Cechak *et al.*, Phys. Lett. B **704**, 24 (2011).
- [32] J. Gasser, V. E. Lyubovitskij, A. Rusetsky and A. Gall, Phys. Rev. D **64**, 016008 (2001); J. Gasser, V. E. Lyubovitskij and A. Rusetsky, Phys. Rept. **456**, 167 (2008); J. Gasser, V. E. Lyubovitskij and A. Rusetsky, Ann. Rev. Nucl. Part. Sci. **59**, 169 (2009) [arXiv:0903.0257 [hep-ph]].
- [33] J. Nieves and E. Ruiz Arriola, Phys. Rev. D **80**, 045023 (2009).
- [34] I. Caprini, G. Colangelo and H. Leutwyler, Phys. Rev. Lett. **96**, 132001 (2006).
- [35] R. Kaminski, J. R. Peláez and F. J. Yndurain, Phys. Rev. D **77**, 054015 (2008).